



Structural Properties of Indium Tin Oxide Thin Films by Glancing Angle Deposition Method

Gyujin Oh, Seon Pil Kim, Kyoung Su Lee, and Eun Kyu Kim*

Quantum-Function Research Laboratory and Department of Physics, Hanyang University,
222 Wangsimni-Ro, Seongdong-Gu, Seoul 133-791, Korea

We have studied the structural and optical properties of indium tin oxide (ITO) films deposited on sapphire substrates by electron beam evaporator with glancing angle deposition method. The ITO films were grown with different deposition angles of 0°, 30°, 45°, 60° at fixed deposition rate of 3 Å/s and with deposition rates of 2 Å/s, 3 Å/s, and 4 Å/s at deposition angle of 45°, respectively. From analysis of ellipsometry measurements, it appears that the void fraction of the films increased and their refractive indices decreased from 2.18 to 1.38 at the wavelength of 500 nm as increasing the deposition angle. The refractive index in the wavelength ranges of 550 nm–800 nm also depends on the deposition rates. Transmittance of ITO film with 235-nm-thickness grown at 60° was covered about 20–80%, and then it was increased in visible wavelength range with increase of deposition angle.

Keywords: Glancing Angle Deposition, Indium Tin Oxide, Antireflection Coating.

1. INTRODUCTION

The advanced optical devices such as light-emitting diode (LED), solar cell, and photo-detector, are required by social needs. Although it is important to improve electrical properties of the devices, there is also significant importance in structural factor of the film surfaces exposed to the environment, which results in devices absorbing broadband or particular wavelength of light with little loss. For penetration of light through thin film, well-adjusted graded index profiles of refractivity minimize Fresnel reflection occurring in the interface of different materials so that it enhances the transmission of light in the every direction.^{1,2} Such modification can be achieved by glancing angle deposition (GLAD) method. The GLAD has been widely studied since first reported in 1959.³ Due to their convenience of controlling the nano-structure of films, there are many attempts to take advantage of it for device fabrication process.^{4–6} When substrates are obliquely exposed to particle flux, it grows the columnar nano-structures containing high porosity, and it makes the films easy to change their refractive properties.^{7–9} The film accumulated by the GLAD method was reported to have various refractive indices along with its porosity.¹⁰ Indium tin oxide (ITO) is a well-known material in fabrication of optical devices for its high transparency and low resistivity.^{11,12} The refractive index of ITO is about 2, so this material can be used for antireflection coatings between air and semiconductor

materials such as GaAs(3.6), Si(3.4), ZnO(1.9), GaN(2.2) and so on. Studies for ITO using an evaporation method have to be implemented in a partial pressure of oxygen gas to keep the stoichiometry of composition of indium, tin, and oxygen elements.^{13–15}

In this study, the structural properties of ITO thin films grown by GLAD method were discussed as a pre-step for further applications to the optical devices. The ITO films were deposited with electron-beam evaporation method without an oxygen flow. Many ITO films with different refractive indices could be fabricated by controllable variables such as the angle between vapor flux and sample holder, and the rotation speed of sample holder.

2. EXPERIMENTAL DETAILS

The ITO films were deposited on sapphire substrates by an *e*-beam evaporation system. Films were prepared to compare physical properties related to deposition rates and deposition angles. The deposition angle means an angle between particle flux and line normal to substrate surface. In this study, the deposition rates were 2 Å/s, 3 Å/s, 4 Å/s, and the deposition angles were 0°, 30°, 45°, 60°, respectively. All films were accumulated to 235-nm-thickness, and then the crystal planes and crystallinity were examined by scanning X-ray diffraction (XRD). Structural properties such as surface morphology and roughness were investigated by an atomic force microscopy (AFM). The ellipsometer confirmed refractive indices, extinction coefficient, and thickness of the films. The void fraction

* Author to whom correspondence should be addressed.

of films was obtained by performing effective medium approximation (EMA) from optical information of ellipsometer. The UV-Vis spectrophotometer verified transmittances of the films.

3. RESULTS AND DISCUSSION

Figure 1 shows XRD patterns for ITO films grown at deposition rate of 3 Å/s on sapphire substrate by *e*-beam evaporation system. Although peak intensity of (222) crystal plane was relatively strong, the diffraction patterns showed entirely broad intensity distribution. Therefore, the film was considered as a more amorphous-like structure.

Figure 2 shows a void fraction in the films deposited at different deposition conditions such as deposition angle and rate, respectively. The void fraction is a measure of void spaces in a material which is able to define a fraction of the volume of voids over the total volume of the material. In this figure, the void fraction in ITO films

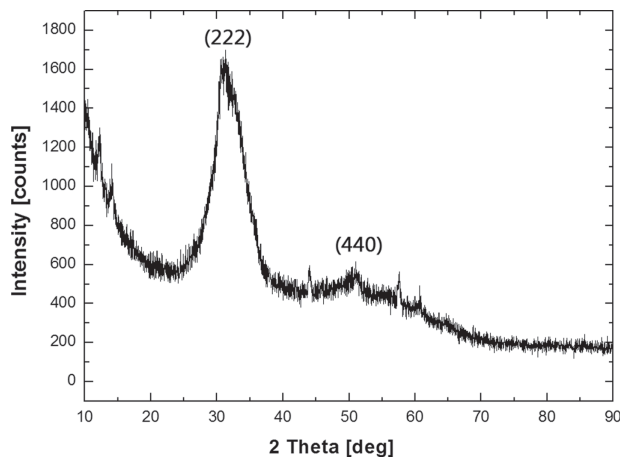


Fig. 1. XRD patterns of the ITO film at deposition rate of 3 Å/s by *e*-beam evaporation system.

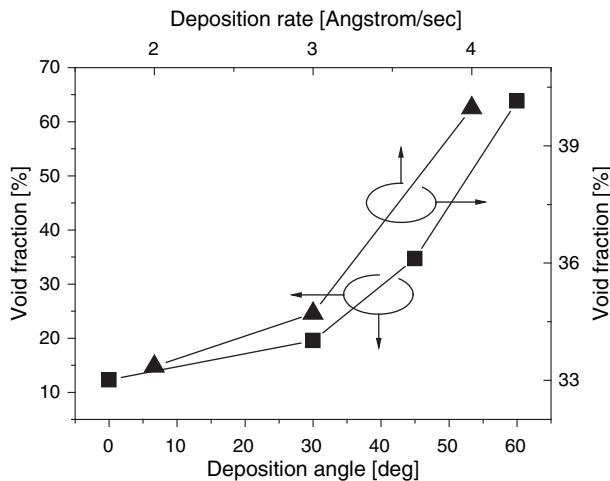


Fig. 2. The void fractions in the ITO films deposited at different deposition angles and rates.

increased up to 65% as deposition angle increased up to 60°. The deposition rate was fixed at 3 Å/s. That was an expected result because GLAD method brings a porous structure by chiefly two mechanisms, limited surface diffusion and shadowing effect. Many precedent reports support this theory with scanning electron microscope images and calculation.¹⁶ On the other hand, when the deposition rates of ITO film increased from 2 Å/s to 4 Å/s, the void fraction increased also from 33% to 40%. Here, the deposition angle was fixed at 45°.

Figures 3(a) and (b) show the refractive index spectra measured by ellipsometer for the ITO films grown at different deposition angles and rates, respectively. The refractive index in the wavelength region from 400 nm to 580 nm decreases gradually as the deposition angle increases, and then it is well consistent with increase of void fraction. The rest of region also showed approximately similar trend. The inset figures show an extinction coefficient of ITO film grown by GLAD. In general, the extinction coefficient will be influenced by the density of ITO films, so the extinction coefficient could be expected to decrease as the void fraction increases. The extinction coefficient roughly coincided with those expectations, and the tendency was most obvious at 45° and 60° angles.

In Figure 3(b), the refractive index spectra for different deposition rates also showed consistent changes on

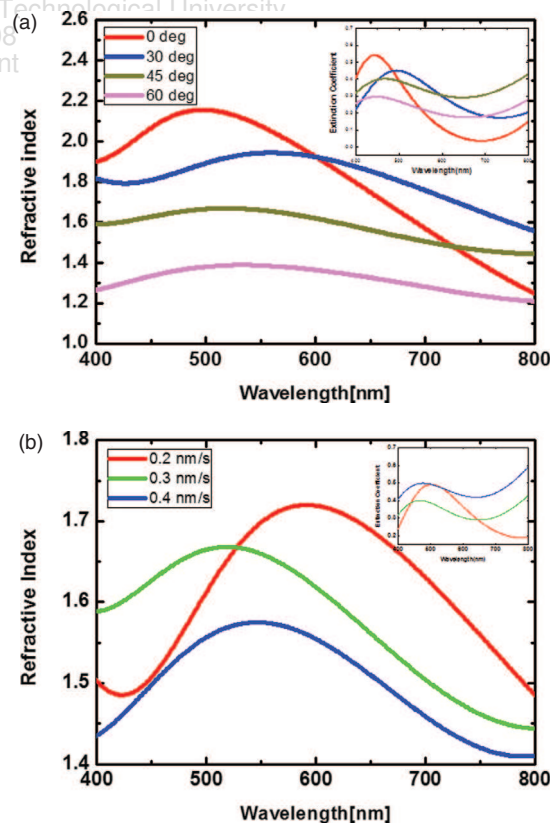


Fig. 3. The refractive index spectra measured by ellipsometer for the ITO films grown at different deposition (a) angles and (b) rates, respectively.

Table I. Optical characteristics at the wavelength of 480 nm and 700 nm for ITO films grown under different deposition angles and different deposition rates, respectively.

Deposition condition	Reflective index	Extinction coefficient	RMS roughness (nm)
Angle at 3 Å/s (480 nm)			
0°	2.14	0.47	5.1
30°	1.86	0.44	4.3
45°	1.65	0.40	5.3
60°	1.37	0.28	7.0
Rate at 45° (700 nm)			
2 Å/s	1.63	0.23	2.9
3 Å/s	1.50	0.31	4.4
4 Å/s	1.46	0.44	4.7

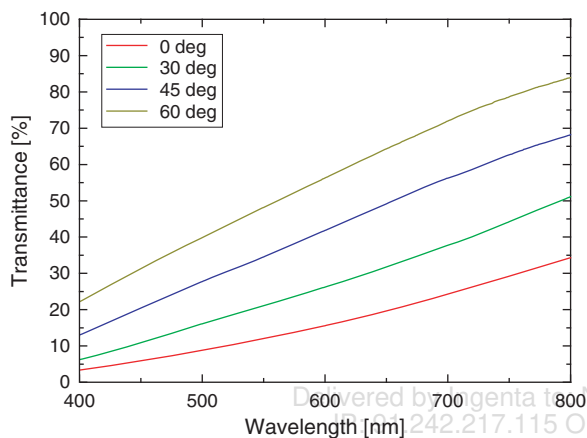


Fig. 4. Optical transmittance spectra for the ITO films with thickness of 235 nm grown at different deposition angles.

the void fraction, especially in the range from 550 nm to 800 nm. The extinction coefficient in the inset figure agreed with the expectation within the wavelength regions of 650-nm to 800-nm-wavelength.

Table I shows the summarized results of RMS roughness obtained by AFM, the optical characteristics such as refractive index and extinction coefficient at the specific wavelength of 480 nm and 700 nm, respectively. As shown in the Table I, the surface roughness values were getting bigger when the deposition angles increase. That result from AFM images qualitatively matches with the void fraction data of Figure 2.

Optical transmittances measured by UV-Vis spectrophotometer was shown in Figure 4. The spectra appeared that how transmittance varies on deposition angles. We could get more obvious tendency compared with extinction coefficient measured by ellipsometer. Here, the transmittance uniformly increased as increasing the deposition angle. However, the transparencies of ITO films grown by GLAD on sapphire substrate appeared to be a lower property compared to commercial ITO thin film. Although XRD peaks coincided with that of typical ITO, the GLAD without

partial pressure of oxygen gas has limitation to make ITO thin films which have high transparency.

4. CONCLUSION

The ITO films were grown on the sapphire substrates by e-beam evaporation with different angles of 0°, 30°, 45°, 60° at fixed deposition rate of 3 Å/s and with deposition rates of 2 Å/s, 3 Å/s, and 4 Å/s at deposition angle of 45°, respectively, and their structural and optical properties were studied. When the angles and rates of deposition were increased, the void fractions of films also increased. Their refractive indices decreased from 2.18 to 1.38 at the wavelength of 500 nm as increasing the deposition angle. The RMS roughness also has a close relationship with void fraction. The effect of void fraction appeared most clearly in transmittance measured by UV-Vis spectrophotometer, and the transmittance of ITO film with 235-nm-thickness grown at 60° deposition angle was covered about 20–80%.

Acknowledgments: This work was supported in part by the Industrial Technology Development Program and Components and Materials Technology Development Program funded by the Ministry of Knowledge Economy, and the NRF of Korea funded by the Ministry of Education, Science and Technology (Grant No. 2012-0003067).

References and Notes

1. J. S. Rayleigh, *Proc. London Math. Soc.* 11, 51 (1880).
2. L. Lu, F. Zhang, Z. Xu, S. Zhao, and Y. Wang, *J. Nanosci. Nanotechnol.* 10, 1723 (2010).
3. N. Young and J. Kowal, *Nature* 183, 104 (1959).
4. S. R. Kennedy and M. J. Brett, *Appl. Opt.* 42, 4573 (2003).
5. P. Chinnamuthu, A. Mondal, N. K. Singh, J. C. Dhar, S. K. Das, and K. K. Chattopadhyay, *J. Nanosci. Nanotechnol.* 12, 6445 (2012).
6. J. K. Kim, S. Chhajed, M. F. Schubert, E. F. Schubert, A. J. Fischer, M. H. Crawford, J. Cho, H. Kim, and C. Sone, *Adv. Mater.* 20, 801 (2008).
7. S.-H. Hong, B.-J. Bae, K.-S. Han, E.-J. Hong, H. Lee, and K.-W. Choi, *Electron. Mater. Lett.* 5, 39 (2009).
8. M. O. Jensen and M. J. Brett, *J. Nanosci. Nanotechnol.* 5, 723 (2005).
9. K. Robbie, J. C. Sit, and M. J. Brett, *J. Vac. Sci. Technol. B* 16, 1115 (1998).
10. J.-Q. Xi, M. F. Schubert, J. K. Kim, E. F. Schubert, M. Chen, S. Lin, W. Liu, and J. A. Smart, *Nature Photon.* 1, 176 (2007).
11. A. W. Sood, D. J. Poxson, F. W. Mont, S. Chhajed, J. Cho, E. F. Schubert, R. E. Welsler, N. K. Dhar, and A. K. Sood, *J. Nanosci. Nanotechnol.* 12, 3950 (2012).
12. K.-K. Kim, H. Kim, S.-N. Lee, and S. Cho, *Electron. Mater. Lett.* 7, 145 (2011).
13. S. Laux, N. Kaiser, A. Zöller, R. Götzelmann, H. Lauth, and H. Bernitzki, *Thin Solid Films* 335, 1 (1998).
14. H.-U. Habermeier, *Thin Solid Films* 80, 157 (1981).
15. H. Kim, C. M. Gilmore, A. Pique, J. S. Horwitz, H. Mattoussi, H. Murata, Z. H. Kafafi, and D. B. Chrisey, *J. Appl. Phys.* 86, 6451 (1999).
16. D. Vick, L. J. Friedrich, S. K. Dew, M. J. Brett, K. Robbie, M. Seto, and T. Smy, *Thin Solid Films* 339, 88 (1999).

Received: 22 October 2012. Accepted: 28 January 2013.